

Premelting and Postmelting in Clusters

Christian Hock,¹ Christof Bartels,¹ Samuel Straßburg,¹ Martin Schmidt,² Hellmut Haberland,¹
Bernd von Issendorff,¹ and Andrés Aguado³

¹Fakultät für Physik, Universität Freiburg, H. Herderstraße 3, 79104 Freiburg, Germany

²Laboratoire Aimé Cotton, F-91405 Orsay, France

³Departamento de Física Teórica, Universidad de Valladolid, Valladolid 47011, Spain

(Received 1 October 2008; published 29 January 2009)

Caloric curves for sodium clusters with $N = 139$ and 147 atoms show a fine structure near the solid-to-liquid transition. Neither of the two sizes exhibit surface melting. For $N = 139$, diffusion of the surface vacancies is observed, which is not possible in the closed-shell $N = 147$ cluster. A few kelvin above the peak in the heat capacity, $N = 139$ is completely liquid. This is not the case for $N = 147$. Here the inner 13 atoms remain nearly fixed up to several tens of kelvin above the melting temperature of the outer two layers. A simple physical reason is suggested for this unexpected behavior.

DOI: 10.1103/PhysRevLett.102.043401

PACS numbers: 36.40.Ei, 36.40.Mr

The solid-to-liquid transition of a large system is the prototype of a classical first-order phase transition and occurs for a given pressure at a fixed temperature T_m^{bulk} . The transition is often simplified as occurring between a perfect crystal and a completely disordered liquid. Actually the story is much richer. Much is known about *premonitory effects* near the melting transition of macroscopic samples [1]. Examples are substantial changes in volume, compressibility, heat capacity, and electric conductivity long before T_m^{bulk} is reached. These effects are mainly due to anharmonic thermal motion and the slow beginning of diffusion. Also, a liquid layer usually forms on a surface before the crystal melts. We show here that related effects happen in clusters.

The calorimeter for free, mass-selected clusters has been discussed earlier [2–8]. Briefly, positively charged sodium clusters are thermalized in a heat bath of temperature T , and mass selected. The clusters absorb several photons from a pulsed laser and the mass spectrum of the photo-fragments is measured. Its temperature dependence allows us to determine the internal energy E , and to construct the caloric curve, $E = E(T)$ [2–8]. Figure 1 shows an example measured with an improved setup [9]. The published melting temperatures [8] have been reproduced to better than 0.5 K. The absolute energy scale in Fig. 1 was obtained by extrapolating the experimental data to $T = E = 0$ using the bulk heat capacity [11].

The simulations were performed using orbital-free *ab initio* isokinetic molecular dynamics [12], where density functional theory is used to calculate the forces acting on the nuclei, whose motion is treated classically. An approximate density functional for the electron kinetic energy leads to a substantial simplification over the Kohn-Sham method, enabling long simulations (up to nearly 2 ns for each temperature) of large samples [13,14]. The calculations were performed on neutral clusters, whereas the experiment has to use charged ones. It is known from previous studies that the number of electrons

does not have a significant effect on the structure and melting of sodium clusters in this size range [2,12–16].

Figure 1 compares the experimental and simulated caloric curves for $N = 147$ sodium atoms. A nearly linear behavior is seen at low temperature, followed by a smooth rise near 260 K, which is due to the increase of phase space near the solid-to-liquid transition. Above the melting temperature T_m (defined here as the temperature corresponding to the maximum slope of the caloric curve) the curves show again a nearly linear increase, with a larger slope than below T_m . Similar data have been published earlier, and

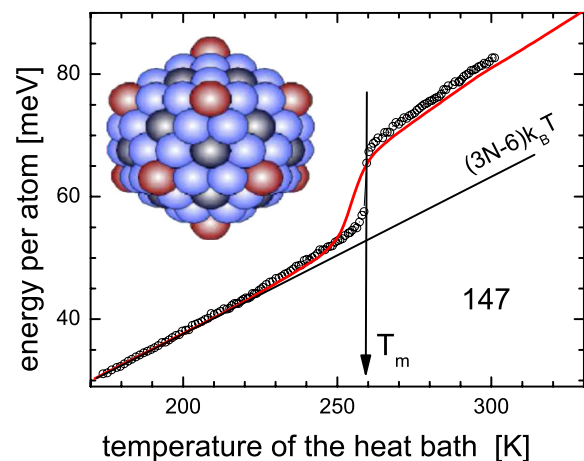


FIG. 1 (color online). Measured (circles) and simulated (solid red line) canonical caloric curves for a sodium cluster with 147 atoms [10]. The straight line indicates the thermal energy of an $N = 147$ atom cluster, whose atoms interact with classical, harmonic forces. The three curves have been normalized to each other at 185 K. The increase near T_m is due to the melting transition. The difference in measured (259.7 K) and simulated (254.4 K) melting temperatures is only 2%. The inset shows the icosahedral structure of the $N = 147$ cluster. There are 12 vertex atoms (red), 60 atoms are on the ridges (blue), while there is only one central atom on the 20 faces (black). The binding energies increase from vertex to ridge to central atoms.

a generally good agreement between experiment and simulation has been obtained [13,14].

Many publications have concentrated on the dominant feature of the caloric curves near T_m : the smooth rise giving the melting temperature and the latent heat of melting [2–8,12–14]. Instead, we will focus here on structures far from T_m which are indicators of the premonitory effects of cluster melting. For an accurate calculation, the simulations had to be carried out for significantly longer times than previously reported [13,14].

The heat capacity is the derivative of the caloric curve, and it is a standard procedure to discuss its fine structure near the melting transition [1,2]. A better diagnostic tool for the experimental data can be obtained by subtracting E^* from the caloric curve, where $E^* = (3N - 6)k_B T$ is the thermal energy of an N -atom cluster in the classical harmonic approximation, and k_B is Boltzmann's constant. The results are given in Figs. 2 and 3. They show an unexpectedly complex melting scenario. The value of T_1 is defined as the lowest temperature at which the average cluster energy departs (within the noise level of the simulations) from the harmonic limit E^* . The statistical error is about 0.1 meV/atom, or $\Delta T = \pm 2$ K.

Experiment and theory [8,13,16] agree that the ground state of Na_{147} is an icosahedron (see Fig. 1). Similarly, Na_{139} is an icosahedron with 8 of the 12 vertex atoms missing [14,16]; this difference will be the key for understanding the differences in the melting behavior.

For $N = 139$ one has $E = E^*$ below $T_1 \sim T_m - 60$ K, with $T_m(\text{expt}) = 259.0$ K, and $T_m(\text{sim}) = 251.4$ K. The simulations clearly show that the increase near T_1 is due to (i) an increasing importance of anharmonic motions (a general effect also observed in simulations of Lennard-Jones (LJ) clusters [17]) and (ii) the diffusion of surface vacancies; i.e., some of the 60 ridge atoms (blue in Fig. 1)

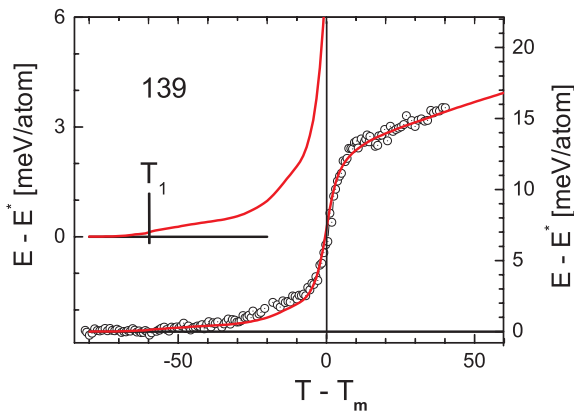


FIG. 2 (color online). The energy $E - E^*$ [$E^* = (3N - 6)k_B T$] is plotted against the deviation from T_m for a cluster of 139 sodium atoms. The solid lines have been simulated. Good agreement is obtained. The left ordinate shows the simulated results on an expanded scale. Above T_1 , anharmonic effects become visible in the cluster energy. Results are collected in Table I.

and the four atoms in vertex positions visit free neighboring places, while the 20 central atoms (black) remain at their positions. This is far from a disordered liquid layer, so this isomerization stage can be called ridge melting, but not premelting [1,14,18].

The slow beginning of the ridge melting can be well seen in the calculated *atomic equivalence indices* (AEI) of Fig. 4 which are 5-ps averages of

$$\sigma_i(t) = \sum_j |\vec{R}_i(t) - \vec{R}_j(t)| \quad (i = 1, \dots, N), \quad (1)$$

where all distances from one atom (i) to all other atoms (j) are summed. If the AEI remain nearly constant, the atoms will not visit neighboring positions. Figure 4 shows that for $N = 139$ some atoms in the outer layer start to become mobile just 10 K above T_1 , or 50 K below T_m .

About 20 K below T_m (or 10 K below T_m for Na_{147}), anharmonicities and thermal expansion increase strongly. The same behavior is observed for the bulk, and it can be considered a premonitory signal for the proximity of the melting point. Just below T_m some subsurface atoms of the $N = 139$ cluster start to fill the surface vacancies, triggering the melting of the whole cluster until about 6 K above T_m all atoms can freely interchange their positions and no apparent structural order remains.

The vacancy-free, icosahedral shape for $N = 147$ generates a different scenario. The isomerization stage is absent as there are no surface vacancies which could diffuse. From Fig. 4 one can deduce that even at 4 K below T_m there is no interchange of atoms, and that no adatom-vacancy pairs are thermally generated. Thus Na_{147} does not exhibit premelting.

Even more surprisingly, similar plots show that up to T_2 in Fig. 3 the central atom remains in its site and its first coordination layer of 12 atoms preserves on average an icosahedral symmetry. Here T_2 is defined as the lowest

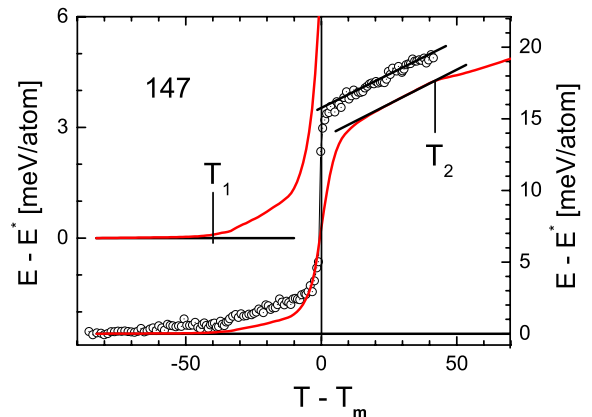


FIG. 3 (color online). As in Fig. 2, but for $N = 147$ sodium atoms. For $T - T_m < 0$ the situation is similar to that for $N = 139$. The temperature T_1 is closer to T_m , as there is no disorder due to diffusing surface vacancies. The simulations show that for $T_m \leq T \leq T_2$ only the two outer atomic layers are liquid and that the inner 13-atom icosahedron remains solid.

TABLE I. Scenario of the melting transition as obtained from the simulations. Below a temperature of T_1 (see Figs. 2 and 3) one has mainly small amplitude harmonic motions. Above T_1 anharmonic effects become more and more important. Only Na_{139} shows ridge melting. Melting starts at $T_m - \delta$, with $\delta = 6 \pm 2$ K. Na_{139} is completely liquid above $T_m + \delta$, while for Na_{147} the central atom and its first coordination layer become mobile only at T_2 .

Cluster	$T \leq T_1$	$T_1 \leq T \leq T_m - \delta$	$\delta + T_m \leq T \leq T_2$	$T_2 \leq T$
$N = 147$ icosahedron	Mainly harmonic motion	Anharmonic motion	Only the outer two layers are molten → postmelting	Liquid
$N = 139$ icosahedron with 8 vertex atoms missing	harmonic motion	As for $N = 147$, plus diffusion of the 8 vacancies of the missing vertex atoms	Liquid	Liquid

temperature at which all atoms in the cluster can diffuse, which correlates with the change of the slope of the caloric curve there [19]. This “postmelting” has not been reported so far [20]. We suggest a simple physical origin: (i) the existence of a nearly vacancy-free, liquid outer shell for $N = 147$ (but *not* 139) up to a few ten kelvin above T_m , and (ii) the large pressure exerted by the surface tension.

In more detail, it is well known that metallic bulk liquids show *surface layering* [21]. The structure of the liquid metal clusters shows the same layering [14], as seen in Fig. 5. The atomic-density oscillations propagate right to the cluster center, and have a larger amplitude for Na_{147} than for Na_{139} ; i.e., the layering is *size dependent*.

Interesting information on the diffusion of atoms above T_m can be obtained from Fig. 5. For $N = 139$ the atomic density is approximately the same in the three density minima, which means that interlayer diffusion is equally

easy between all shells. On the other hand, the atomic density for $N = 147$ in the interlayer regions decreases significantly when approaching the core region. In particular, the innermost atom never diffuses at this temperature, and the minimum separating the 13-atom icosahedral core and the rest of the cluster is also rather low; i.e., there are only occasional interchanges of one of those 12 atoms with the external shells, as typical of a solid-liquid interface, and icosahedral order is preserved.

Only a few, short-lived adatom-vacancy pairs are thermally generated for $T_m < T < T_2$ in the outer liquid layer of Na_{147} , so that this layer can support the large pressure p resulting from the surface tension σ and prevent the 13-atom icosahedral core from melting. One can get a rough value for p from the Laplace pressure $p = 2\sigma/R$, where $R \sim 1$ nm is the radius of Na_{147} . Taking the bulk value of $\sigma = 0.26 \text{ J m}^{-2}$ [22] gives about 5000 bar. A similar value is obtained from the simulations [19]. This leads to a

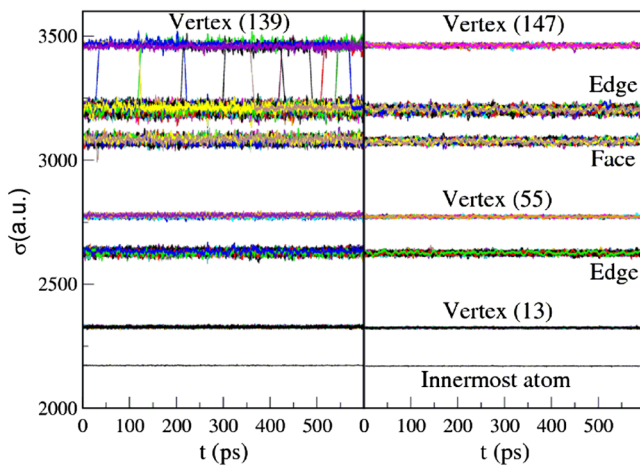


FIG. 4 (color online). Calculated atomic equivalence indices in atomic units (a.u.). At left for $N = 139$ at $T_m - 50$ K, and at right for $N = 147$ at $T_m - 4$ K [see Eq. (1)]. The AEI lines are generally broader for $N = 139$, which indicates larger vibrational amplitudes; they also show motion of atoms in the outer shell. No interchange of atoms can be seen for $N = 147$; thus, there is no diffusion so close to T_m in this case. The numbers in parentheses give the total number of atoms up to the first, second, or third shell, respectively.

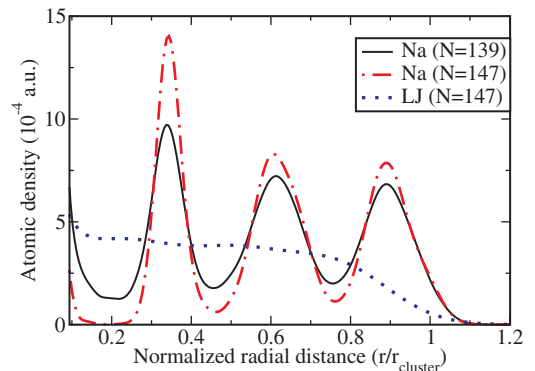


FIG. 5 (color online). The calculated atomic radial density is plotted against the normalized distance r/r_{cluster} , where r is the distance from the cluster center of mass and r_{cluster} is defined here as the radius which contains 95% of the cluster mass. The two Na results are for a temperature of 270 K which is above T_m but below T_2 ; i.e., the inner core for $N = 147$ is still solid. The atomic layering can be clearly seen. Note that the first minimum for Na_{147} touches the r axis, indicating that the central atom does not diffuse at this temperature, a clear indicator of postmelting. A Lennard-Jones (LJ) cluster just above its T_m , on the other hand, shows no layering at all [19,24].

pressure-induced increase of T_m by about 40–50 K according to the bulk Na phase diagram [23], correlating well with the T_2 given in Fig. 3.

Although the Laplace pressure is very similar in both clusters, postmelting is not observed for $N = 139$. At and above T_m , the less compact surface facilitates radial atomic diffusion, as seen in Fig. 5. The resulting strong fluctuations lead—via the Lindemann criterion [2]—to a melting of the inner core just above T_m . Some remnants of postmelting behavior can be seen very close to T_m if one inspects the calculated trajectories: At $T_m + 3$ K it takes up to 400 ps on average for the innermost atom to exchange its position with another atom. But this happens so close to T_m that its influence on the caloric curve is masked by the much larger contribution of the latent heat of melting.

We conjecture that postmelting should be quite general for metal clusters with a compact surface shell, as no sodium-specific properties have been used in the argument. Note also that layering is not observed in nonmetallic surfaces [21]; thus, postmelting is not expected to occur in these cases (see Fig. 5 for a LJ cluster). The postmelting scenario is presently only supported by the calculations. Some experimental data [9] seem to indicate a small change of slope in the predicted temperature range, but no clear statement can be made presently.

In summary, a joint experimental and theoretical study was done on the melting of sodium clusters containing 139 and 147 atoms, respectively. The simulations give a complete physical picture of the transition; in particular, the influence of anharmonic motion is seen several tens of kelvin below the melting temperature of the cluster. Neither of the clusters exhibit surface melting below T_m ; the only disorder appearing here is a diffusion of the surface vacancies along the ridges in Na_{139} , which is not possible for $N = 147$ due to its closed-shell icosahedral shape. While Na_{139} becomes completely liquid a few kelvin above the main transition temperature, Na_{147} exhibits extended postmelting, with its central 13-atom icosahedron remaining solid up to 40 K above T_m .

We thank Michael Moseler for discussions. This research was supported by the Deutsche Forschungsgemeinschaft, Junta de Castilla y León, the Spanish MEC, and the European Regional Development Fund (Projects FIS2008-02490/FIS and GR120).

[1] J.G. Dash, *Contemp. Phys.* **43**, 427 (2002); A.R. Ubbelohde, *Melting and Crystal Structure* (Clarendon, Oxford, 1965); J.G. Dash, H. Fu, and J.S. Wettlaufer, *Rep. Prog. Phys.* **58**, 115 (1995). R.M. Feenstra *et al.*, *Phys. Rev. Lett.* **66**, 3257 (1991).

[2] For a review on cluster melting, see F. Baletto and R. Ferrando, *Rev. Mod. Phys.* **77**, 371 (2005).

[3] M. Schmidt, R. Kusche, B. v. Issendorff, and H. Haberland, *Nature (London)* **393**, 238 (1998).

[4] A description of the experiment and the data evaluation can be found in H. Haberland, in *Proceedings of the Les*

Houches Summer School, Session 73, edited by C. Guet *et al.* (Springer, Heidelberg, 2001), p. 29.

[5] A review of the thermodynamic results of the Freiburg group up to 2002 can be found in M. Schmidt and H. Haberland, and C.R. *Physique* **3**, 327 (2002).

[6] M. Schmidt, J. Donges, Th. Hippler, and H. Haberland, *Phys. Rev. Lett.* **90** 103401 (2003).

[7] M. Schmidt, R. Kusche, Th. Hippler, J. Donges, W. Kronmüller, B. von Issendorff, and H. Haberland, *Phys. Rev. Lett.* **86**, 1191 (2001).

[8] H. Haberland, Th. Hippler, J. Donges, O. Kostko, M. Schmidt, and B. von Issendorff, *Phys. Rev. Lett.* **94**, 035701 (2005).

[9] Christian Hock, Ph.D. thesis, Universität Freiburg (unpublished).

[10] The expensive first-principles simulation cannot be made completely ergodic very near to T_m , although each separate run was carried out for almost 2 ns. Even longer simulations can change the caloric curves near T_m a bit but not several 10 K away, where the premonitory effects occur which are discussed here. A canonical evaluation was used for the experimental data [4]; therefore, the S-like shape (backbending) as observed earlier [7] for $N = 147$ is not seen in Fig. 1.

[11] Ralph Hultgren, *Selected Values of the Thermodynamic Properties of the Elements* (American Society for Metals, Metals Park, OH, 1973).

[12] A. Aguado *et al.*, in *Trends in Chemical Physics Research*, edited by A.N. Linke (Nova Science, New York, 2005), Ch. 10, p. 205.

[13] A. Aguado and J.M. López, *Phys. Rev. Lett.* **94**, 233401 (2005).

[14] A. Aguado, *J. Phys. Chem. B* **109**, 13043 (2005); E.G. Noya, J.P.K. Doye, D.J. Wales, and A. Aguado, *Eur. Phys. J. D* **43**, 57 (2007).

[15] A.K. Starace, C.M. Neal, B. Cao, M.F. Jarrold, A. Aguado, and J.M. López, *J. Chem. Phys.* **129**, 144702 (2008).

[16] O. Kostko, B. Huber, M. Moseler, and B. von Issendorff, *Phys. Rev. Lett.* **98**, 043401 (2007).

[17] J.P.K. Doye and D.J. Wales, *J. Chem. Phys.* **102**, 9659 (1995).

[18] Features in the heat capacity of Al clusters have been interpreted as being due to premelting; see G.A. Breaux, C.M. Neal, B. Cao, and M.F. Jarrold, *Phys. Rev. Lett.* **94**, 173401 (2005).

[19] A. Aguado (unpublished).

[20] Premelting occurs below T_m [1,18]. In analogy, the term postmelting is coined here, as it concerns a feature with a temperature higher than T_m .

[21] Several physical reasons are offered in the literature for surface layering. The one prevailing nowadays is that it is a general phenomenon for all materials having a wide liquid stability range, that is, a large difference between the melting and boiling temperatures. This happens for metals but not, e.g., for Lennard-Jones systems. E. Chacón *et al.*, *Phys. Rev. Lett.* **87**, 166101 (2001); O.G. Shpyrko *et al.*, *Science* **313**, 77 (2006).

[22] A.R. Miedema and R. Boom, *Z. Metallkd.* **69**, 183 (1978).

[23] C.S. Zha and R. Boehler, *Phys. Rev. B* **31**, 3199 (1985).

[24] F.H. Stillinger and D.K. Stillinger, *J. Chem. Phys.* **93**, 6013 (1990).